Neutron-neutron and neutron-photon correlations with FREYA

R. Vogt[1,2,a] and J. Randrup[3,b]

[1] Lawrence Livermore National Laboratory, Livermore, CA 94551, USA
[2] Physics Department, University of California at Davis, Davis, CA 95616, USA
[3] Nuclear Science Division, Lawrence Berkeley National Laboratory, Berkeley, CA 94720, USA

Abstract. For many years, the state of the art for modeling fission in radiation transport codes has involved sampling from average distributions. However, in a true fission event, the energies, momenta and multiplicities of emitted particles are correlated. The FREYA (Fission Reaction Event Yield Algorithm) code generates complete fission events. Event-by-event techniques such as those of FREYA are particularly useful because it is possible to obtain complete kinematic information on the prompt neutrons and photons emitted during the fission process. It is therefore possible to extract any desired correlation observables. We describe FREYA and compare our results with neutron-neutron, neutron-light fragment and neutron-photon correlation data.

1. Introduction to FREYA

The computational model FREYA [1–7] generates complete fission events, *i.e.* it provides the the full kinematic information on the two product nuclei as well as all the emitted neutrons and photons. In its development, an emphasis had been put on speed, so large event samples can be generated fast, and FREYA therefore relies on experimental data supplemented by simple physics-based modeling. In its standard version, to treat a given fission case, FREYA needs the fission fragment mass distribution $Y(A)$ and the total kinetic energy TKE(A) for the particular excitation energy considered. $Y(A)$ is taken either directly as the measured yields or as a five-Gaussian fit to the data which makes it possible to parametrize its energy dependence [3].

In order to generate an event, FREYA first selects the mass split based on $Y(A)$. The fragment charges are then sampled from the normal distributions suggested by experiment [3]. The linear and angular momenta of the two fragments and their internal excitations are subsequently sampled. After their formation, the fully accelerated fragments de-excite first by neutron evaporation and then by photon emission. In addition to spontaneous fission, FREYA treats neutron-induced fission up to $E_n = 20\,\mathrm{MeV}$; the possibility of pre-fission evaporation is considered as well as pre-equilibrium neutron emission (which plays a role at the highest energies).

FREYA contains a number of adjustable parameters that control various physics aspects:

- dTKE an overall shift of $\overline{\mathrm{TKE}}$ relative to the input TKE(A), used to adjust to the average neutron multiplicity $\overline{\nu}$;
- e_0 the overall scale of the Fermi-gas level density parameters;
- x the advantage in excitation energy given to the light fragment;
- c_S the ratio of the 'spin temperature' to the 'scission temperature';
- c_T the relative statistical fluctuation in the fragment excitations;
- Q_{min} the energy above the neutron separation threshold where photon emission takes over from neutron emission;
- t_{max} the maximum half-life of a level during the photon decay process which stops when the level half-life exceeds t_{max}.

For a given split of nucleus A_0 into light and heavy fragments, L and H respectively, the Q-value is given by $Q = M_0c^2 - M_Lc^2 - M_Hc^2$. For a given total fragment kinetic energy TKE, the energy available for rotational and statistical excitation of the two fragments is then $E^*_{\mathrm{sc}} = Q - \overline{\mathrm{TKE}}$ and the corresponding scission temperature T_{sc} is obtained from $E^*_{\mathrm{sc}} = (A_0/e_0)T^2_{\mathrm{sc}}$.

The inclusion of angular momentum in FREYA was described in Ref. [6]. The overall rigid rotation of the dinuclear configuration prior to scission, caused by the absorption of the incoming neutron and the recoil(s) from any evaporated neutron(s), dictates certain mean angular momenta in the two fragments. In addition, due to the statistical excitation of scission, the fragments also acquire fluctuations around those mean values. FREYA includes fluctuations in the wriggling and bending modes (consisting of rotations in the same or opposite sense around an axis perpendicular to the dinuclear axis) but ignores tilting and twisting (in which the fragments rotate around the dinuclear axis). These dinuclear rotational modes are assumed to become statistically excited during scission and are thus described by Boltzmann distributions,

$$P_{\pm}(\mathrm{s}_{\pm})\, ds^x_{\pm} ds^y_{\pm} \sim \exp(-s^2_{\pm}/2\mathcal{I}_{\pm}T_S) ds^x_{\pm} ds^y_{\pm}, \qquad (1)$$

where $\mathrm{s}_{\pm} = (s^x_{\pm}, s^y_{\pm}, 0)$ is the spin of the normal modes with plus referring to the wriggling modes (having parallel rotations) and minus referring to the bending modes (having opposite rotations). The corresponding moments

[a] e-mail: vogt2@llnl.gov
[b] e-mail: jrandrup@lbl.gov

of inertia are denoted $\mathcal{I}_\pm$ [4,6]. The degree of fluctuation is governed by the 'spin temperature' $T_S = c_S T_{\rm sc}$ which can be adjusted by means of the parameter c_S. The fluctuations vanish for $c_S = 0$ so the fragments emerge with the angular momenta dictated by the overall rigid rotation of the scission configuration (usually very small for induced fission and absent for spontaneous fission). The default value, $c_S = 1$, gives $\overline{S}_L \sim 6.2\hbar$ and $\overline{S}_H \sim 7.6\hbar$ for ^{252}Cf(sf) and provides reasonable agreement with the average energy of photons emitted in fission [6].

After accounting for the total rotational energy of the two fragments, $E_{\rm rot}$, we are left with a total of $E_{\rm stat} = E^*_{\rm sc} - E_{\rm rot}$ for statistical fragment excitation that is distributed between the two fragments. First a preliminary partition, $E_{\rm stat} = \acute{E}^*_L + \acute{E}^*_H$, is made according to the heat capacities of the two fragments which are assumed to be proportional to the corresponding Fermi-gas level density parameters, *i.e.* $\acute{E}^*_L : \acute{E}^*_H = a_L : a_H$, where

$$a_i(\acute{E}^*_i) = \frac{A_i}{e_0}\left[1 + \left(\frac{\delta W_i}{U_i}\right)(1 - \exp(-\gamma U_i))\right] \qquad (2)$$

with $U_i = \acute{E}^*_i - \Delta_i$ and $\gamma = 0.05/\text{MeV}$ [8]. The pairing energy of the fragment, Δ_i, and its shell correction, δW_i, are tabulated in Ref. [8] based on the mass formula of Koura et al. [9]. The overall scale e_0 is taken as a model parameter but it should be noted that if the shell corrections are negligible, $\delta W_i \approx 0$, or the available energy, U_i, is large, then $a_i \approx A_i/e_0$, *i.e.* a_i is simply proportional to the fragment mass number A_i, and this renormalization is immaterial. We take $e_0 \sim 10/\text{MeV}$ [3]. If the two fragments are in mutual thermal equilibrium, $T_L = T_H$, the total excitation energy will, on average, be partitioned as above. But because the observed neutron multiplicities suggest that the light fragments tend to be disproportionately excited, the average excitations are modified in favor of the light fragment,

$$\overline{E}^*_L = x\,\acute{E}^*_L \ , \ \overline{E}^*_H = E_{\rm stat} - \overline{E}^*_L \qquad (3)$$

where x is expected be larger than unity. It was found that $x = 1.3$ leads to reasonable agreement with $\nu(A)$ for ^{252}Cf(sf), while $x = 1.2$ is suitable for ^{235}U(n,f) [2].

After the mean fragment excitation energies have been assigned as described above, FREYA considers the effect of thermal fluctuations. In Weisskopf's statistical model of the nucleus, which describes the excited nucleus as a degenerate Fermi gas, the mean excitation of a fragment is related to its temperature T_i by $\overline{E}^*_i = \tilde{a}_i T_i^2$ and the associated variance in the excitation is

$$\sigma^2_{E_i} = -\partial^2 \ln \rho_i(E_i)/\partial E_i^2 = 2\overline{E}^*_i T_i \ . \qquad (4)$$

Therefore, for each of the two fragments, we sample an energy fluctuation δE^*_i from a normal distribution of variance $2c_T \overline{E}^*_i T_i$ and adjust the fragment excitations accordingly, arriving at $E^*_i = \overline{E}^*_i + \delta E^*_i$, $i = L, H$. Energy conservation is accounted for by making a compensating opposite fluctuation in the total kinetic energy,

$$\text{TKE} = \overline{\text{TKE}} - \delta E^*_L - \delta E^*_H \ . \qquad (5)$$

The average TKE, $\overline{\text{TKE}}$, has been adjusted by dTKE to reproduce the average neutron multiplicity, $\overline{\nu}$. The factor c_T multiplying the variance was introduced to explore the effect of the truncation of the normal distribution at the maximum available excitation. Its value affects the neutron multiplicity distribution $P(\nu)$. We have used $c_T = 1.0$ as a default but it can be adjusted to $P(\nu)$.

The evaporated neutrons are assumed to be isotropic (in the frame of the emitting nucleus), apart from a very slight flattening due to the nuclear rotation. Their energy is sampled from a black-body spectrum,

$$\frac{dN_n}{dE_n} \sim E_n \exp(-E_n/T_{\rm max}), \qquad (6)$$

where $T_{\rm max}$ is the maximum possible temperature in the daughter nucleus, corresponding to very soft neutron emission. FREYA generally assumes that neutron evaporation continues until the nuclear excitation energy is below the threshold $S_n + Q_{\rm min}$, where S_n is the neutron separation energy and $Q_{\rm min} = 0.01\,\text{MeV}$ so that neutron evaporation continues as long as energetically possible.

After neutron evaporation has ceased, the excited product nucleus will undergo sequential photon emission which is treated in several stages. The most recent refinement uses the RIPL-3 data library [10] for the discrete decays towards the end of the decay chain. The first stage is statistical radiation. These photons are emitted isotropically with an energy that has been sampled from a black-body spectrum modulated by a giant-dipole resonance form factor,

$$\frac{dN_\gamma}{dE_\gamma} \sim \frac{\Gamma^2_{\rm GDR} E^2_\gamma}{(E^2_\gamma - E^2_{\rm GDR})^2 - \Gamma^2_{\rm GDR} E^2_\gamma} E^2_\gamma \exp(-E_\gamma/T). \qquad (7)$$

The position of the resonance is taken as $E_{\rm GDR}/\text{MeV} = 31.2/A^{1/3} + 20.6/A^{1/6}$ [11], while its width is $\Gamma_{\rm GDR} = 5\,\text{MeV}$. Each emission is assumed to reduce the magnitude of the angular momentum by $dS = 1\,\hbar$.

This cascade continues until the statistical excitation is below a specified threshold, $\epsilon_{\rm min}$, which is usually taken to be $\epsilon_{\rm min} = 100\,\text{keV}$. At this point the nucleus is near its yrast line, *i.e.* it is cold and rotating, and the remaining de-excitation occurs by emission of 'collective' photons that each reduce the angular momentum by $2\,\hbar$. The RIPL-3 library [10] tabulates a large number of discrete electromagnetic transitions for nuclei throughout the nuclear chart, but complete information is available for only relatively few of them. However, by making certain assumptions, it is possible to construct, for each product species, a table of the level energies $\{\varepsilon_\ell\}$, their half-lives $\{t_\ell\}$, and the branching ratios of the decays of the lowest levels. Whenever the decay process leads to an excitation below any of the tabulated levels, FREYA switches to a discrete cascade based on the RIPL-3 data. Discrete emission is continued until the half-life t_ℓ exceeds the value of *e.g.* the detector response time $t_{\rm max}$.

2. Results

Two examples of correlated neutron results with FREYA are now discussed. In Fig. 1 two-neutron correlations are compared with data from Ref. [12]. Two-neutron angular correlations result in a characteristic shape with peaks at $\theta_{nn} = 0$ and 180°. The peak at $\theta_{nn} = 0$ occurs when

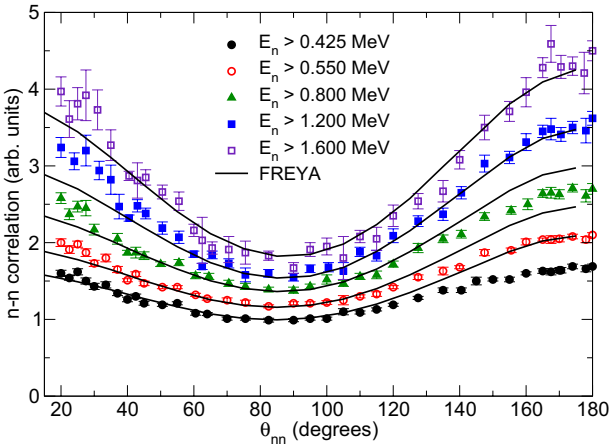

Figure 1. FREYA calculations of two-neutron angular correlations are compared to data from Ref. [12]. See Ref. [5] for full details.

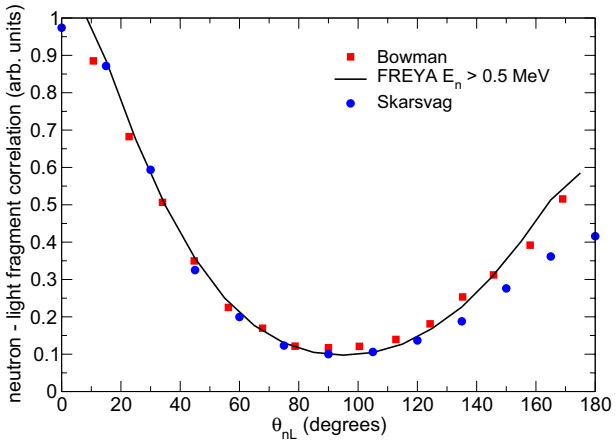

Figure 2. FREYA calculations are compared to ^{252}Cf(sf) neutron-light fragment correlation data from [14] (red squares) and [15] (blue circles). The minimum kinetic energy of the neutrons is 0.5 MeV.

both neutrons are emitted by the same fragment. If both neutrons are emitted by the light fragment, the 0° peak is higher. The peak at 180° arises when one neutron is emitted by each fragment. Even though the neutrons are emitted isotropically in the fragment rest frame, the boost to the lab frame assures that the neutrons follow the parent fragments. The neutron multiplicity affects the correlations: the higher ν, the weaker the correlation [2]. See Refs. [5, 13] for other comparisons to neutron-neutron correlation data.

Neutrons can also be correlated with a particular fragment. Bowman et al. presented the angular correlation between all measured neutrons and the identified light fragment. While the correlation is made with the light fragment, it was not possible to determine which fragment emitted the neutron [14]. In FREYA, if all neutrons come from the light fragment, there is a strong peak at $\theta_{nLF} = 0$ with essentially no signal in the opposite direction. This is because the neutrons will follow the parent fragment due to the boost. Likewise, if all detected neutrons arise from the heavy fragment, the correlation is effectively reflected around $\theta_{nLF} = 90°$. The shape of the correlation from all emitted neutrons retains the largest peak at zero degrees while, in the backward direction, the signal is reduced. This is because more neutrons are emitted by the light fragment because it gets more intrinsic excitation energy. The model results are compared to the Bowman et al. [14] and Skarsvag and Bergheim [15] data in Fig. 2. The agreement of our correlation with the shape of the data is very good. See Ref. [5] for more details.

Photon emission is not boosted so that photon emission is isotropic independent of frame. Thus neutron-photon and two-photon angular correlations are independent of the relative angle. To determine these correlations, other observables must be sought.

The results in Fig. 3 shows one type of neutron-photon correlation, the ratio of the photon to neutron multiplicity for a given fragment mass. The FREYA calculation, not including the discrete cascade, has structure similar to the data from Ref. [16] but differs in magnitude. There is a peak in both results near the doubly-closed shell at $A = 132$, the location of the minimum of the sawtooth in $\nu(A)$. Thus there is no trivial correlation between neutron and photon emission.

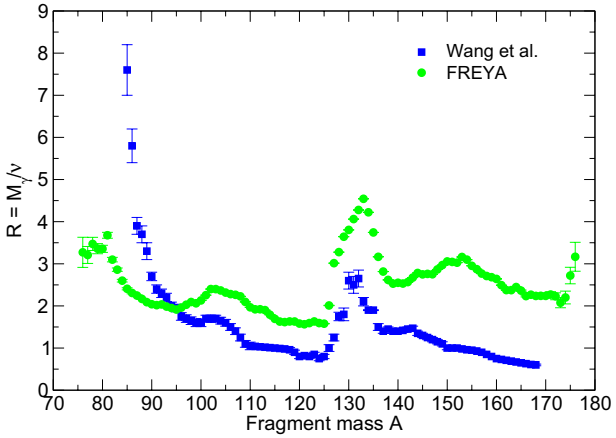

Figure 3. The ratio of photon to neutron multiplicity as a function of fragment mass is compared to data. See Ref. [16] for more details.

In Ref. [16], the photon multiplicity was also plotted against neutron multiplicity in three different fragment mass regions representing the light fragment, the region around symmetric splits, and the heavy fragment. Given the A region, the data were binned in TKE. A slight positive correlation was observed for the light fragment while a somewhat steeper slope was seen in the symmetric region. However, the data showed a more complex behavior in the heavy fragment region. The FREYA calculations showed a small positive slope in all mass regions. We have yet to compare our results with the RIPL-3 lines included to these data. For full results, see Ref. [16].

3. Summary

We have shown that event-by-event models of fission, such as FREYA, provide a powerful tool for studying correlations in fission. The calculations are robust, being relatively insensitive to the input parameters which can be constrained by other data. The agreement of our neutron correlation calculations with the available data is good and does not lend strong support for the requirement of scission neutrons to explain the correlations. However, further data on these correlations based on fission of other isotopes

and, for neutron-induced fission, at higher incident neutron energies would be welcome to help verify these results.

While the agreement of our neutron-photon correlation calculations shown here with the data from Ref. [16] is not as good, the results are promising. Since they were obtained before the RIPL-3 lines were added to FREYA, perhaps further improvement is possible.

The work of R.V. was performed under the auspices of the U.S. Department of Energy by Lawrence Livermore National Laboratory under Contract DE-AC52-07NA27344. The work of J.R. was performed under the auspices of the U.S. Department of Energy by Lawrence Berkeley National Laboratory under Contract DE-AC02-05CH11231. The authors also thank the United States Department of Energy National Nuclear Security Administration Office of Defense Nuclear Nonproliferation Research and Development for support for this work.

References

[1] J. Randrup and R. Vogt, Phys. Rev. C **80**, 024601 (2009)
[2] R. Vogt and J. Randrup, Phys. Rev. C **84**, 044621 (2011)
[3] R. Vogt, J. Randrup, D.A. Brown, M.A. Descalle, and W.E. Ormand Phys. Rev. C **85**, 024608 (2012)
[4] R. Vogt and J. Randrup, Phys. Rev. C **87**, 044602 (2013)
[5] R. Vogt and J. Randrup, Phys. Rev. C **90**, 064623 (2014)
[6] J. Randrup and R. Vogt Phys. Rev. C **89**, 044601 (2014)
[7] J. Randrup and R. Vogt, in progress
[8] T. Kawano, private communication
[9] H. Koura, M. Uno, T. Tachibana and M. Yamada, Nucl. Phys. A **674**, 47 (2000)
[10] R. Capote et al., Nucl. Data Sheets **110**, 3107 (2009)
[11] B.L. Berman and S.C. Fultz, Rev. Mod. Phys. **47**, 713 (1975)
[12] A.M. Gagarski et al., Bull. Russ. Acad. Sciences: Physics, **72**, 773 (2008)
[13] S.A. Pozzi et al, Nucl. Sci. Eng. **178**, 1 (2014)
[14] H.R. Bowman, J.C.D. Milton, S.G. Thompson, and W.J. Swiatecki, Phys. Rev. **126**, 2120 (1962); Phys. Rev. **129**, 2133 (1963)
[15] K. Skarsvag and K. Bergheim, Nucl. Phys. **45**, 72 (1963)
[16] T.F. Wang, G. Li, L. Zhu, Q. Meng, L. Wang, H. Han, W. Zhang, H. Xia, L. Hou, R. Vogt, and J. Randrup, Phys. Rev. C **93**, 014606 (2016)